Impact of in-plane anisotropic strains on the dielectric and pyroelectric properties of $Ba_{0.7}Sr_{0.3}TiO_3$ thin films

Hai-Xia Cao[a)]
Department of Applied Physics, The Hong Kong Polytechnic University, Hong Kong, China and Department of Physics, Suzhou University, Suzhou 215006, China

Veng Cheong Lo
Department of Applied Physics, The Hong Kong Polytechnic University, Hong Kong, China

Zhen-Ya Li
CCAST (World Laboratory), P.O. Box 8730, Beijing 100080, China and Department of Physics, Suzhou University, Suzhou 215006, China

(Received 18 July 2006; accepted 29 October 2006; published online 11 January 2007)

A modified Landau-Devonshire phenomenological thermodynamic theory is used to describe the influence of in-plane anisotropic strains on the dielectric and pyroelectric properties of epitaxial $Ba_{0.7}Sr_{0.3}TiO_3$ thin films grown on dissimilar tetragonal substrates. The in-plane anisotropic strain factor-temperature phase diagram is developed. The in-plane anisotropic strains play a crucial role in the dielectric and pyroelectric properties of BST thin films. The theoretical maximum dielectric tunability approaching 100% can be attained at the critical anisotropic strain factor corresponding to the structural phase transformation from ca_1 to a_1 phase. Moreover, the anisotropic strain factor has an opposite effect on the figure of merit and pyroelectric coefficient, respectively. Furthermore, in the case of isotropic strains, our theoretical results are well consistent with the experimental results.
 [DOI: 10.1063/1.2407272]

I. INTRODUCTION

During the past decade, ferroelectric thin films have been extensively investigated due to their physical properties and promising applications in various fields of microelectronics. In particular, $Ba_{1-x}Sr_xTiO_3$ (BST) thin films have long been recognized as the potential candidates for use in tunable microwave devices such as phase shifter, bandpass filter, and delay line, as well as the well-known capacitor applications such as storage capacitor in dynamic random access memory and decoupling capacitor integrated into monolithic circuit.[1–3] These applications rely strongly on the excellent ferroelectric and dielectric properties of BST films including a high dielectric permittivity, reasonably low dielectric loss, and high dielectric tunability.[4–6] The dielectric tunability (i.e., the degree of variation in dielectric permittivity as a function of applied electric field) is one of the key design parameters of tunable microwave devices. It is desirable to accomplish a large tunability with a small dielectric loss. On the other hand, the application of ferroelectric materials in infrared detectors is still important, such as economical pyroelectric detectors and thermal imaging devices. One major advantage is that they can operate at room temperature, thereby eliminating the need for expensive cooling systems.[7–10] Moreover, the integration of hybrid arrays of ferroelectric thin films detectors with silicon readout integrated circuits can offer high-performance infrared imaging. BST thin films are also considered as the candidate materials for pyroelectric sensors because of their relatively large nonlinear pyroelectric response at room temperature, good reliability, good sensitivity, and low cost.

The fundamental problem that limits the use of BST films is that they have inferior dielectric and pyroelectric properties compared to their bulk counterparts, which are usually ascribed to compositional and microstructural inhomogeneities, defects, and internal strains. In homogeneous epitaxial single-domain ferroelectric thin films, internal strains arise due to various reasons, including the lattice mismatch between the film and the substrate, the difference in thermal expansion coefficients of the film and the substrate, the self-strain induced by the paraelectric-ferroelectric phase transformation, and defects such as dislocations and vacancies. Although such strains often lead to degradation of film properties, if judicious use is made of substrates and growth parameters, strains can offer the opportunity to enhance particular properties of a chosen material in thin film form, namely, strain engineering.[11,12] A great progress has been achieved in the experimental study of the isotropic misfit strain effect, induced in the ferroelectric thin films grown on cubic substrates.[13–16] The internal strains have a pronounced impact on the dielectric and pyroelectric behaviors of BST thin films through the electrostrictive effect and phase transitions. It has been shown that the dielectric permittivity and the pyroelectric coefficient of epitaxial BST thin films can be tuned by varying the misfit strain. The misfit strain can be controlled through the selection of a substrate material and by the variation of the film thickness. Besides, if the ferroelectric thin films are grown on tetragonal or orthorhombic substrates, the misfit strain along a crystalline axis will obviously differ from that along the other crystalline axis, which is called anisotropic misfit strains. Recent experiments have demonstrated that the in-plane anisotropic strain can be induced in $(Pb,Sr)TiO_3$ thin film by using orthorhombic

[a)]Electronic mail: hxcao@suda.edu.cn

$NdGaO_3$ (110) as a substrate and may significantly affect dielectric properties of the film.[17] Moreover, in-plane dielectric properties of ⟨110⟩ oriented epitaxial $(Ba_{0.60}Sr_{0.40})TiO_3$ thin films have been experimentally studied under the influence of anisotropic epitaxial strains from ⟨100⟩ $NdGaO_3$ substrates.[18,19] The anisotropic misfit strains may result in different material properties and thus open up other possibilities for the design of electronic devices.

With the advancement of experimental techniques, BST films with different composition ratios Ba/Sr were fabricated by a variety of thin film deposition techniques including rf-magnetron sputtering, sol-gel, metal-organic chemical vapor deposition (MOCVD), and laser ablation process.[20–22] Theoretically, phase diagrams and dielectric and pyroelectric responses of epitaxial BST films were investigated within the framework of a Landau-Devonshire phenomenological model.[23] In addition, optimization of the tunability of BST films via epitaxial stresses was analyzed using a phenomenological model. However, the previous experimental and theoretical works were only concentrated on the effect of in-plane isotropic strains on the thermodynamic properties of BST thin films. Up to now, the influence of in-plane anisotropic strains on the phase diagram and dielectric and pyroelectric responses of BST films has not been studied theoretically. Consequently, the aim of this work is to investigate the impact of in-plane anisotropic strains on the dielectric tunability and pyroelectric response of $Ba_{0.7}Sr_{0.3}TiO_3$ thin films grown on dissimilar substrates by developing the Landau-Devonshire-type phenomenological thermodynamic theory. This theory was recently employed to predict the equilibrium polarization states and dielectric properties of $BaTiO_3$ and $PbTiO_3$ thin films.[24,25] The strontium composition of $x=0.30$ is the most widely investigated composition because its Curie temperature is very close to room temperature ($T_C=34\ ^\circ C$) and the dielectric permittivity is large enough. A deep understanding of the relationship between the anisotropic strains and the material properties will provide guidelines on how to control the material properties by manipulating the anisotropic strains, which might be crucial for applications of BST thin films.

II. THEORETICAL DEVELOPMENT

Suppose a single-domain $Ba_{0.7}Sr_{0.3}TiO_3$ thin film epitaxially grown in the (001) oriented cubic paraelectric state on a thick tetragonal substrate. If the thickness of the substrate is much larger than the film thickness, the internal stresses are concentrated in the film and the substrate is stress-free. For such a configuration, the in-plane anisotropic misfit strains can be calculated as $u_{m1}=(a_1-a_f)/a_1$ and $u_{m2}=(a_2-a_f)/a_2$, where a_1 and a_2 are the in-plane lattice parameters along the two different crystalline axes and a_f the lattice constant of the cubic paraelectric phase at the stress-free state. When $u_{m1(2)}>0$, it is a tensile strain, and when $u_{m1(2)}<0$, it is compressive. The in-plane shear strain is approximately taken as zero because of the tetragonal thick substrate. We introduce an anisotropic strain factor $\beta=u_{m2}/u_{m1}$, which denotes the extent of anisotropy. The thermodynamic description may be developed starting from the power-series expansion of the modified Landau-Devonshire thermodynamic potential $\tilde{G}$ in terms of polarization component $P_i(i=1,2,3)$, in-plane strain u_{m1}, anisotropic strain actor β, and applied field $E_i(i=1,2,3)$. The relevant general expression for this expansion reads[23–25]

$$\begin{aligned}\tilde{G} = {} & \alpha_1^* P_1^2 + \alpha_2^* P_2^2 + \alpha_3^* P_3^2 + \alpha_{11}^* (P_1^4 + P_2^4) + \alpha_{33}^* P_3^4 + \alpha_{12}^* P_1^2 P_2^2 + \alpha_{13}^* (P_2^2 P_3^2 + P_1^2 P_3^2) \\ & + \alpha_{111}(P_1^6 + P_2^6 + P_3^6) + \alpha_{112}[P_1^4(P_2^2 + P_3^2) + P_2^4(P_1^2 + P_3^2) + P_3^4(P_1^2 + P_2^2)] + \alpha_{123} P_1^2 P_2^2 P_3^2 \\ & + \frac{s_{11}u_{m1}^2(1+\beta) - 2s_{12}u_{m1}^2\beta}{s_{11}^2 - s_{12}^2} - E_1P_1 - E_2P_2 - E_3P_3. \end{aligned} \tag{1}$$

The vector and tensor quantities are defined in a Cartesian coordinate system, for example, $P_1 \| [100]$, $P_2 \| [010]$, and $P_3 \| [001]$. The renormalized coefficients of the free energy expansion in Eq. (1) are

$$\alpha_1^* = \alpha_1 - \frac{Q_{12}u_{m1}(s_{11}\beta - s_{12}) + Q_{11}u_{m1}(s_{11} - s_{12}\beta)}{s_{11}^2 - s_{12}^2},$$

$$\alpha_2^* = \alpha_1 - \frac{Q_{12}u_{m1}(s_{11} - s_{12}\beta) + Q_{11}u_{m1}(s_{11}\beta - s_{12})}{s_{11}^2 - s_{12}^2},$$

$$\alpha_3^* = \alpha_1 - \frac{Q_{12}u_{m1}(1+\beta)}{s_{11}+s_{12}},$$

$$\alpha_{11}^* = \alpha_{11} + \frac{1}{2(s_{11}^2 - s_{12}^2)}[(Q_{11}^2 + Q_{12}^2)s_{11} - 2Q_{11}Q_{12}s_{12}],$$

$$\alpha_{12}^* = \alpha_{12} - \frac{1}{s_{11}^2 - s_{12}^2}[(Q_{11}^2 + Q_{12}^2)s_{12} - 2Q_{11}Q_{12}s_{11}] + \frac{Q_{44}^2}{2s_{44}},$$

$$\alpha_{13}^* = \alpha_{12} + \frac{Q_{12}(Q_{11}+Q_{12})}{s_{11}+s_{12}},$$

$$\alpha_{33}^* = \alpha_{11} + \frac{Q_{12}^2}{s_{11}+s_{12}}, \tag{2}$$

where α_1 is the dielectric stiffness, α_{ij} and α_{ijk} are higher order stiffness coefficients at constant stress, Q_{ij} are the elec-

trostrictive coefficients, and s_{ij} the elastic compliances of the film. The temperature dependence of the dielectric stiffness α_1 is given by the Curie-Weiss law, $\alpha_1=(T-T_0)/2\varepsilon_0 C$, where T_0 and C are the Curie-Weiss temperature and constant of a bulk ferroelectrics, respectively, and ε_0 is the permittivity of free space.

The polarization components as a function of the applied field can be derived from the Landau-Devonshire thermodynamic potential using the stability criterion of the first partial derivative ($\partial\tilde{G}/\partial P_i=0$), as shown below.

$$\alpha_1^* P_1 + 2\alpha_{11}^* P_1^3 + \alpha_{12}^* P_1 P_2^2 + \alpha_{13}^* P_1 P_3^2 - \frac{E_1}{2} = 0, \tag{3}$$

$$\alpha_2^* P_2 + 2\alpha_{11}^* P_2^3 + \alpha_{12}^* P_1^2 P_2 + \alpha_{13}^* P_2 P_3^2 - \frac{E_2}{2} = 0, \tag{4}$$

$$\alpha_3^* P_3 + 2\alpha_{33}^* P_3^3 + \alpha_{13}^* (P_1^2 + P_2^2) P_3 - \frac{E_3}{2} = 0, \tag{5}$$

where the contribution of sixth-order polarization terms to the thermodynamic potential is neglected. The electric field dependent relative dielectric permittivities along [100], [010], and [001] directions can be determined by

$$\frac{\varepsilon_{11}(E_1)}{\varepsilon_0} = \left(\varepsilon_0 \frac{\partial^2 \tilde{G}}{\partial P_1^2}\right)^{-1} = \frac{1}{2\varepsilon_0[\alpha_1^* + 6\alpha_{11}^* P_1^2 + \alpha_{12}^* P_2^2 + \alpha_{13}^* P_3^2]}, \tag{6}$$

$$\frac{\varepsilon_{22}(E_2)}{\varepsilon_0} = \left(\varepsilon_0 \frac{\partial^2 \tilde{G}}{\partial P_2^2}\right)^{-1} = \frac{1}{2\varepsilon_0[\alpha_2^* + 6\alpha_{11}^* P_2^2 + \alpha_{12}^* P_1^2 + \alpha_{13}^* P_3^2]}, \tag{7}$$

and

$$\frac{\varepsilon_{33}(E_3)}{\varepsilon_0} = \left(\varepsilon_0 \frac{\partial^2 \tilde{G}}{\partial P_3^2}\right)^{-1} = \frac{1}{2\varepsilon_0[\alpha_3^* + 6\alpha_{33}^* P_3^2 + \alpha_{13}^* (P_1^2 + P_2^2)]}, \tag{8}$$

respectively. The small-signal dielectric response along [100], [010], and [001] directions can also be determined by Eqs. (6)–(8) with the polarizations given by setting E_i equal to zero in Eqs. (3)–(5). Correspondingly, we define the dielectric tunability Φ as the variation in the dielectric response with the applied field with respect to the small-signal dielectric permittivity as

$$\Phi = \begin{cases} 1-\varepsilon_{11}(E_1)/\varepsilon_{11}(E_1=0) & \text{for } E_1 \| [100] \\ 1-\varepsilon_{22}(E_2)/\varepsilon_{22}(E_2=0) & \text{for } E_2 \| [010] \\ 1-\varepsilon_{33}(E_3)/\varepsilon_{33}(E_3=0) & \text{for } E_3 \| [001]. \end{cases} \tag{9}$$

In the presence of a uniform applied electric field E_3 normal to the film substrate interface, the pyroelectric coefficient p_3 is given as the sum of the variations of the spontaneous polarization and the dielectric permittivity $\varepsilon_{33}(E_3)$ with the temperature,

$$p_3 = \left| \frac{\partial P_3}{\partial T} + E_3 \frac{\partial \varepsilon_{33}(E_3)}{\partial T} \right|. \tag{10}$$

TABLE I. The parameters for the calculation of the renormalized coefficients for $Ba_{0.7}Sr_{0.3}TiO_3$ films.

Parameter	$Ba_{0.7}Sr_{0.3}TiO_3$
Curie temperature T_C (°C)	34
Curie constant C (10^5 °C)	1.29
α_{11} (10^6 m^5/C^2 F)	$2.52T+189$ (Tin°C)
α_{12} (10^8 m^5/C^2 F)	7.21
s_{11} (10^{-12} m^2/N)	5.92
s_{12} (10^{-12} m^2/N)	−1.92
s_{44} (10^{-12} m^2/N)	6.7
Q_{11} (m^4/C^2)	0.1
Q_{12} (m^4/C^2)	−0.034
Q_{44} (m^4/C^2)	0.029

III. NUMERICAL RESULTS AND DISCUSSION

The effect of in-plane anisotropic strains on the phase diagram, dielectric tunability, and pyroelectric response in epitaxial $Ba_{0.7}Sr_{0.3}TiO_3$ thin films is discussed in this section. The parameters for the calculation of the renormalized coefficients for $Ba_{0.7}Sr_{0.3}TiO_3$ thin films are obtained by averaging the corresponding parameters of $BaTiO_3$ and $SrTiO_3$ materials shown in Table I.[23] Both α_1 and α_{11} are temperature dependent in $Ba_{0.7}Sr_{0.3}TiO_3$ films since both are scaled with temperature in $BaTiO_3$, and the other parameters are assumed to be temperature independent.

In order to describe the transformations of equilibrium thermodynamic states that may occur in epitaxial $Ba_{0.7}Sr_{0.3}TiO_3$ films in the presence of in-plane anisotropic strains, it is useful to develop a misfit strain-temperature phase diagram. Figure 1 illustrates the anisotropic strain factor-temperature phase diagram for $Ba_{0.7}Sr_{0.3}TiO_3$ films under the short-circuited condition, at a given in-plane misfit strain $u_{m1}=0.002$. The equilibrium thermodynamic states of the film are determined by calculating all minima of the potential $\tilde{G}$ with respect to polarization components and then selecting the most energetically favorable phase. The presence of anisotropic strains may strongly affect the thermodynamic stability of various phases involved. The formation of six distinct phases due to the change in the symmetry as a result of the in-plane anisotropic misfit strains is predicted theoretically. These six phases are the paraelectric phase ($P_1=P_2=P_3=0$), the c phase ($P_1=P_2=0$, $P_3\neq 0$), the a_1 phase ($P_1\neq 0$, $P_2=P_3=0$), the a_2 phase ($P_2\neq 0$, $P_1=P_3=0$), the ca_1 phase ($P_1\neq 0$, $P_2=0$, $P_3\neq 0$), and the a_1a_2 phase ($P_1\neq 0$, $P_2\neq 0$, $P_3=0$). Because of the in-plane anisotropic strains, the paraelectric-to-ferroelectric transition temperature has a plateau above the a_1 phase, which is similar to the case of $BaTiO_3$ thin films with the in-plane anisotropic strains.[25] This phenomenon is different from the "seagull" shape of the transition temperature versus the isotropic strains. It is interesting to see that the significant feature in-

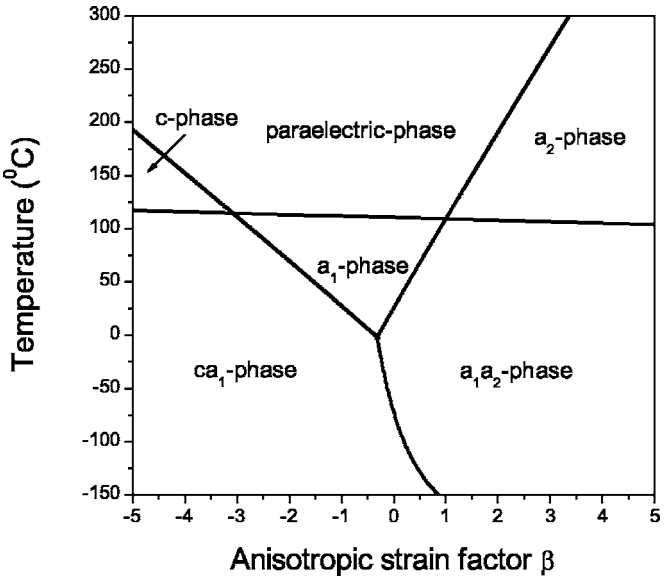

FIG. 1. The anisotropic strain factor-temperature phase diagram for $Ba_{0.7}Sr_{0.3}TiO_3$ thin films under the short-circuited condition, at a given in-plane misfit strain $u_{m1}=0.002$.

duced by the anisotropic strains is the formation of the tetragonal ferroelectric phases, a_1 and a_2, which do not exist in the BST films of the same composition in the presence of isotropic strains. Under a fixed tensile strain u_{m1}, the a_2 phase is stable when the tensile strain u_{m2} is large enough, and the a_1 phase is stable when u_{m2} is either a small tensile or a small compressive strain. This indicates that the anisotropic strains may alter the type of the stable ferroelectric phase. Compared with the phase diagram of $BaTiO_3$ thin films under the anisotropic misfit strains,[25] Fig. 1 reveals that the c phase occurs when the one in-plane strain is tensile and the other is compressive in epitaxial $Ba_{0.7}Sr_{0.3}TiO_3$ films. On the other hand, the used fourth-order Landau-Devonshire polynomial cannot describe the thermodynamic properties of bulk BST at a lower temperature with the given parameters since α_{11} becomes negative at a lower temperature. Consequently, the corresponding Fig. 1 cannot be extended to a temperature below −190 °C.

Since the anisotropic strain-induced phase transitions may be accompanied by dielectric and pyroelectric anomalies, we discuss the impact of anisotropic strain factor on the dielectric and pyroelectric responses of $Ba_{0.7}Sr_{0.3}TiO_3$ films. A thorough examination of Fig. 1 reveals that only the ca_1, a_1, and a_1a_2 phases are the stable phases at room temperature (25 °C). The room temperature dielectric tunability of $Ba_{0.7}Sr_{0.3}TiO_3$ films along [100], [010], and [001] with applied fields along the same directions is calculated by using the definition of the dielectric tunability [Eq. (9)] and the dielectric response as a function of the applied field [Eqs. (6)–(8)]. The maximum applied field is taken as 100 kV/cm for $E\|[100]$, [010], and [001], respectively. Figure 2 demonstrates the dielectric tunability as a function of anisotropic strain factor at $T=25$ °C and $u_{m1}=0.002$, (a) and (b) corresponding to the ca_1 phase and the a_1a_2 phase, respectively. It can be clearly seen that the dielectric tunability strongly depends on the anisotropic strain factor. For the ca_1 phase, as

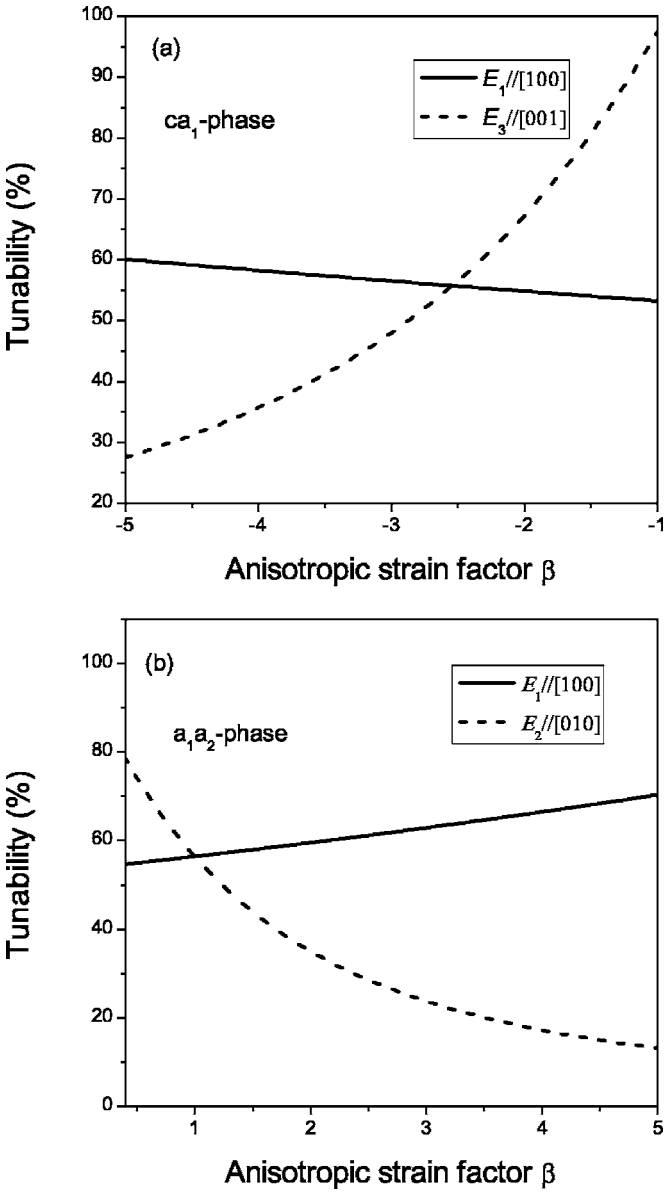

FIG. 2. The variation of the dielectric tunability along the different external fields as a function of the anisotropic strain factor at $T=25$ °C and $u_{m1}=0.002$, (a) and (b) corresponding to the ca_1 phase and the a_1a_2 phase, respectively.

shown in Fig. 2(a), the dielectric tunability along [100] linearly decreases, but the dielectric tunability along [001] nonlinearly increases, with decreasing the magnitude of the anisotropic strain factor. In addition, the theoretical maximum dielectric tunability approaching 100% can be attained at the critical anisotropic strain factor corresponding to the structural phase transformation from the ca_1 phase to the a_1 phase. Figure 2(b) displays the effect of anisotropic strain factor on the in-plane dielectric tunability. The dielectric tunability along [100] linearly increases, but the one along [010] nonlinearly decreases with the increase of the anisotropic strain factor. In the vicinity of the phase transformations from the a_1 phase to the a_1a_2 phase, the dielectric tunability along [100] has the minimum dielectric tunability, but the corresponding value along [010] has the maximum one close

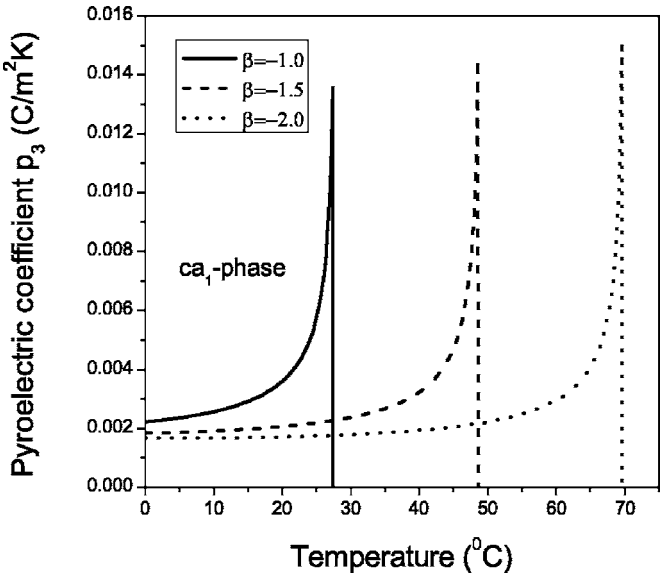

FIG. 3. The dependence of the out-of-plane pyroelectric coefficient in the ca_1 phase on the temperature for a fixed $u_{m1}=0.002$ and different anisotropic factors ($\beta=-1.0,-1.5,-2.0$).

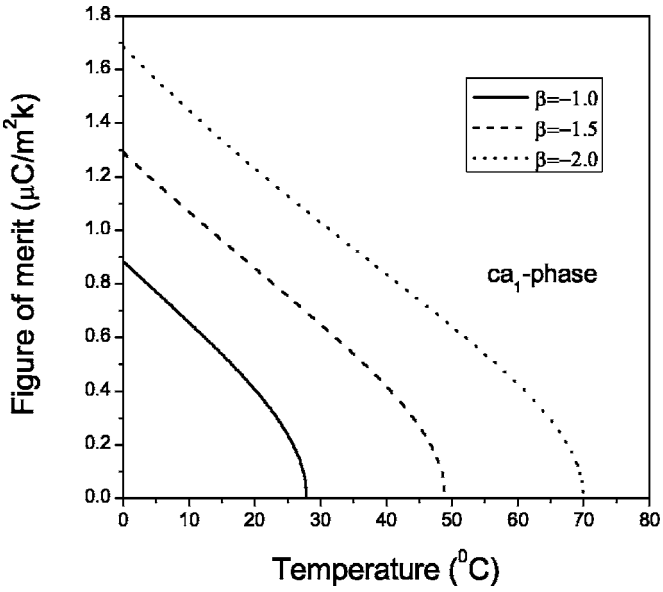

FIG. 4. The figure of merit as a function of temperature for a given $u_{m1}=0.002$ and different anisotropic strain factors ($\beta=-1.0,-1.5,-2.0$).

to 80%. This indicates that the dielectric tunability can be optimized by modulating the in-plane anisotropic strains and varying the ferroelectric states.

The a_1a_2 phase and the a_1 phase at room temperature are not suitable for applications in infrared sensors due to their in-plane polarizations. We only focus on the impact of anisotropic strain factors on the pyroelectric response along [001] in the ca_1 phase state, which is a more favorable state for the application in the pyroelectric sensors. Theoretical investigation has shown that the external field has little influence on the pyroelectric coefficient because of the overwhelming contribution of spontaneous polarization to the overall pyroelectric coefficient, so we do not take the external field into consideration.[23] In the ca_1 phase, the out-of-plane pyroelectric coefficient as a function of temperature for a fixed $u_{m1}=0.002$ and different anisotropic factors ($\beta=-1.0$, -1.5, -2.0) is shown in Fig. 3. For a given anisotropic strain factor, the pyroelectric coefficient increases with temperature, and then a pyroelectric coefficient peak appears in the vicinity of the phase transformation from the ca_1 phase to the a_1 phase. In addition, the peak value of the pyroelectric coefficient shifts to a higher temperature on increasing anisotropic factor. For a given temperature, the out-of-plane pyroelectric coefficient can be effectively improved by decreasing the magnitude of the anisotropic strain factor. Therefore, we can optimize the pyroelectric response by modulating the anisotropic strain factor. In a real application for infrared sensors, the figure of merit is more important than the pyroelectric coefficient itself. Increasing the figure of merit is an effective method to improve the pyroelectric performance of a pyroelectric device. In the ca_1 phase, the figure of merit F is defined as $F=p_3/\varepsilon_{33}$, where p_3 is the out-of-plane pyroelectric coefficient and ε_{33} is the dielectric permittivity along [001]. In Fig. 4, the figure of merit as a function of temperature for a given $u_{m1}=0.002$ and different anisotropic strain factors ($\beta=-1.0$, -1.5, -2.0) is depicted. Compared with Fig. 3, Fig. 4 exhibits that the effects of anisotropic strain factor on the figure of merit and pyroelectric coefficient are opposite. For a given anisotropic strain factor, the figure of merit decreases with the increase of the temperature. Besides, for a fixed temperature, the figure of merit can be improved by increasing the magnitude of the anisotropic strain factor. It is nevertheless worth noticing that, in the experimental research, the selection of the substrate and the film thickness can be chosen as design parameters to manipulate the internal in-plane anisotropic strain level to achieve optimum pyroelectric response.

In order to compare the predictions with experimental results,[26] we also calculate the in-plane dielectric permittivity ε_{11} as a function of external field under the different strains $u_{m1}=0.001,0.0016,0.003$ and a temperature $T=25$ °C, in the case of the in-plane isotropic strains ($\beta=1.0$), as depicted in Fig. 5. The in-plane isotropic strains can be regarded as a particular case of in-plane anisotropic strain distribution states. For a given temperature, the dielectric permittivity increases on decreasing the tensile strain. Besides, the influence of in-plane isotropic strain on the in-plane dielectric permittivity is more obvious when the external field is small. Interestingly, when the in-plane isotropic strain $u_{m1}=0.0016$, our theoretical prediction of the in-plane dielectric permittivity for $Ba_{0.7}Sr_{0.3}TiO_3$ films is in good agreement with the experimental results published in the literature (see Ref. 26), as shown by the solid diamonds in the Fig. 5. Wang *et al.* prepared the $Ba_{0.7}Sr_{0.3}TiO_3$ films grown on MgO (001) single-crystal substrate using pulsed-laser deposition and obtained the enhanced in-plane ferroelectricity.[26] According to the experimental data, the calculated maximum in-plane dielectric tunability is 67.87% under a moderate dc bias field of 13.3 V/μm. Our theoretical result is 66.43% under the in-plane strain $u_{m1}=0.0016$, which is well consistent with the experimental result. It should be noted that the calculated lattice misfit strain is $u_{\text{lattice}}=0.041\,94$, according to the lattice constants of MgO substrate and $Ba_{0.7}Sr_{0.3}TiO_3$ film, 0.4211 and 0.40344 nm, respectively. On the other hand, as

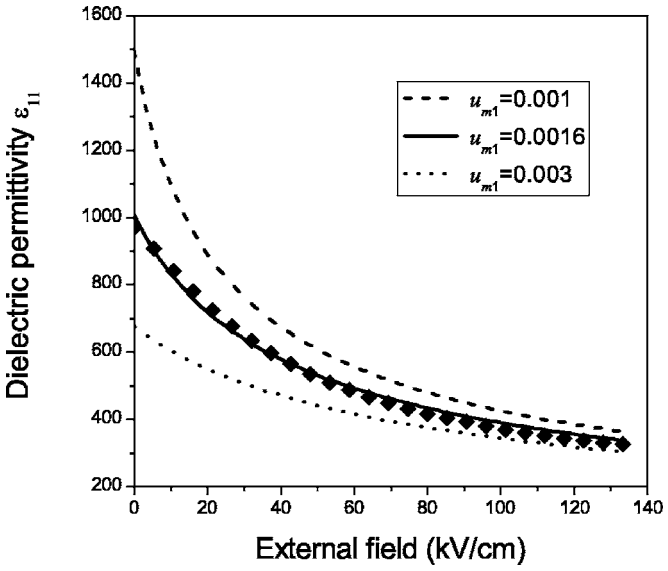

FIG. 5. The in-plane dielectric permittivity ε_{11} as a function of external field under the different strains $u_{m1}=0.001, 0.0016, 0.003$ and a temperature $T=25\ ^{\circ}\mathrm{C}$, in the case of the in-plane biaxial isotropic strains ($\beta=1.0$). The solid diamonds are experimental data from Ref. 26.

the film is cooled from growth temperature T_G, the thermal strain can be calculated from the following expression:

$$u_{\text{thermal}} = \int_{T}^{T_G} (\alpha_{\text{film}} - \alpha_{\text{substrate}})dt, \tag{11}$$

where α_{film} and $\alpha_{\text{substrate}}$ are the thermal expansion coefficients of the $Ba_{0.7}Sr_{0.3}TiO_3$ thin film and the MgO substrate, respectively. According to Eq. (11), for $\alpha_{\text{film}}=10.5\times10^{-6}\ ^{\circ}\mathrm{C}^{-1}$ and $\alpha_{\text{substrate}}=13.47\times10^{-6}\ ^{\circ}\mathrm{C}^{-1}$, the calculated thermal strain is $u_{\text{thermal}}=-0.002\,15$. We can get $u_{m1}<(u_{\text{lattice}}+u_{\text{thermal}})$, which means that the actual internal strain level is not only related to the misfit strain and the thermal strain but also dependent on the other factors, such as oxygen defect, film inhomogenity, surface electrode, etc. Besides, the epitaxial strains are relaxed to a certain extent by the formation of misfit dislocations at T_G, which is related to the film thickness.[27] The formation of misfit dislocations can play an important role in decreasing the internal strain level of BST thin films in the experiment.

IV. CONCLUSION

In summary, we have developed a modified thermodynamic model based on the Landau-Devonshire-type phenomenological theory to investigate the impact of in-plane anisotropic strains on the dielectric and pyroelectric responses in epitaxial $Ba_{0.7}Sr_{0.3}TiO_3$ thin films. The anisotropic strain factor-temperature phase diagram has been established. The significant feature induced by the anisotropic strains is the formation of the tetragonal ferroelectric phases, a_1 and a_2, which do not exist in the BST films of the same composition under isotropic strains. In addition, the influence of anisotropic strain factor on the dielectric tunability, the pyroelectric coefficient, and the figure of merit is analyzed. The calculated results demonstrate that the in-plane anisotropic strains play an important role in the dielectric and pyroelectric properties of BST thin films. The theoretical maximum dielectric tunability approaching 100% can be attained at the critical anisotropic strain factor corresponding to the structural phase transformation from the ca_1 phase to the a_1 phase. The anisotropic strain factor has opposite effect on the figure of merit and the pyroelectric coefficient, respectively. The out-of-plane pyroelectric coefficient can be effectively improved, but the figure of merit decreases, by decreasing the magnitude of the anisotropic strain factor. Moreover, we have also studied the effect of biaxial isotropic strain on the in-plane dielectric permittivity and the dielectric tunability in order to compare with the experimental results. When the biaxial isotropic strain $u_{m1}=0.0016$, our theoretical results are well consistent with the experimental results. On the whole, the theoretical insight into the impact of in-plane anisotropic strains on the dielectric and pyroelectric properties of BST thin films will undoubtedly provide an instructive clue for the experimental researchers on how to enhance the dielectric tunability and pyroelectric response of the BST thin films.

ACKNOWLEDGMENTS

This work was supported by the Research Grant of the Hong Kong Polytechnic University under Grant No. G-U032, the National Natural Science Foundation of China under Grant Nos. 10547129, 10174049, and 10474069, and the Natural Science Foundation of JiangSu Education Committee of China under the Grant No. 04KJB140118.

[1] K. Morito and T. Suzuki, J. Appl. Phys. **97**, 104107 (2005).
[2] S. Hyun and K. Char, Appl. Phys. Lett. **79**, 254 (2001).
[3] C. L. Canedy, H. Li, S. P. Alpay, L. Salamanca-Riba, A. L. Royburd, and R. Ramesh, Appl. Phys. Lett. **77**, 1695 (2000).
[4] R. Plonka, R. Dittmann, N. A. Pertsev, E. Vasco, and R. Waser, Appl. Phys. Lett. **86**, 202908 (2005).
[5] N. K. Pervez, P. J. Hansen, and R. A. York, Appl. Phys. Lett. **85**, 4451 (2004).
[6] B. H. Park, Y. Gim, Y. Fan, Q. X. Jia, and P. Lu, Appl. Phys. Lett. **77**, 2587 (2000).
[7] Z. T. Song, N. Chong, H. L. W. Chan, and C. L. Choy, Appl. Phys. Lett. **79**, 668 (2001).
[8] Z.-G. Ban and S. P. Alpay, Appl. Phys. Lett. **82**, 3499 (2003).
[9] A. Sharma, Z.-G. Ban, and S. P. Alpay, Appl. Phys. Lett. **84**, 4959 (2004).
[10] A. Sharma, Z.-G. Ban, S. P. Alpay, and J. V. Mantese, J. Appl. Phys. **95**, 3618 (2004).
[11] K. J. Choi *et al.*, Science **306**, 1005 (2004)..
[12] J. H. Haeni *et al.*, Nature (London) **430**, 758 (2004).
[13] Y. I. Yuzyuk, P. Simon, I. N. Zakharchenko, V. A. Alyoshin, and E. V. Svividov, Phys. Rev. B **66**, 052103 (2002).
[14] W. Y. Park, K. H. Ahn, and C. S. Hwang, Appl. Phys. Lett. **83**, 4387 (2003).
[15] T. R. Taylor, P. J. Hansen, B. Acikel, N. Pervez, R. A. York, S. K. Streiffer, and J. S. Speck, Appl. Phys. Lett. **80**, 1978 (2002).
[16] H. Li, A. L. Roytburd, S. P. Alpay, T. D. Tran, L. Salamanca-Riba, and R. Ramesh, Appl. Phys. Lett. **78**, 2354 (2001).
[17] Y. Lin, X. Chen, S. W. Liu, C. L. Chen, J. S. Lee, Y. Li, Q. X. Jia, and A. Bhalla, Appl. Phys. Lett. **84**, 577 (2004).
[18] W. K. Simon, E. K. Akdogan, A. Safari, and J. A. Bellotti, Appl. Phys. Lett. **87**, 082906 (2005).
[19] W. K. Simon, E. K. Akdogan, and A. Safari, J. Appl. Phys. **97**, 103530 (2005).
[20] H. Wang, S. Nien, and K. Lee, Appl. Phys. Lett. **84**, 2874 (2004).
[21] N. A. Suvorava, C. M. Lopez, E. A. Irene, A. A. Suvorova, and M. Saunders, J. Appl. Phys. **95**, 2672 (2004).
[22] J. Lee, Y. Li, Y. Lin, S. Y. Lee, and Q. X. Jia, Appl. Phys. Lett. **84**, 3825 (2004).

[23]Z.-G. Ban and S. P. Alpay, J. Appl. Phys. **91**, 9288 (2002); **93**, 504 (2003).
[24]A. G. Zembilgotov, N. A. Pertsev, U. Böttger, and R. Waser, Appl. Phys. Lett. **86**, 052903 (2005).
[25]J. Wang and T. Y. Zhang, Appl. Phys. Lett. **86**, 192905 (2005).
[26]D. Y. Wang, Y. Wang, X. Y. Zhou, H. L. W. Chan, and C. L. Choy, Appl. Phys. Lett. **86**, 212904 (2005).
[27]V. Nagarajan, C. L. Jia, H. Kohlstedt, R. Waser, I. B. Misirlioglu, S. P. Alpay, and R. Ramesh, Appl. Phys. Lett. **86**, 192910 (2005).